Elucidation of Factors Affecting the Electronic Structures of Magnesium(II) and Zinc(II) Tetraarylporphyrin Radical Cations

Claudia M. Barzilay, Sharon A. Sibilia, Thomas G. Spiro, and Zeev Gross*

Abstract: A series of magnesium and zinc tetraarylporphyrins and their porphyrin-oxidized derivatives were studied by UV/Vis, ESR, and resonance Raman spectroscopy at various temperatures. The series included tetra(*meta*-dichlorophenyl)porphyrinatozinc (**5**), tetra(*ortho*-dichlorophenyl)porphyrinatozinc (**6**), tetra(*ortho*-difluorophenyl)porphyrinatozinc and -magnesium (**9** and **10**), and tetra(pentafluorophenyl)porphyrinatozinc and -magnesium (**7** and **8**). The radical cations (**3a**–**10a**) were isolated by chemical one-electron oxidation of their neutral precursors (**3**–**10**). Despite the structural similarity of all these radicals, their electronic ground state varied within the series. The position of the chloro groups was found to play a key role. While the radical cation of the *meta*-dichloro-substituted derivative **5a** exhibited A_{2u} spectroscopic features, the *ortho*-dichlorophenyl derivative (**6a**) showed A_{1u} spectral features. Radicals of the fluoro-substituted porphyrins, especially that of **10**, were found to have state-admixed (A_{1u}/A_{2u}) electronic structures, and the relative contributions of the two states was found to vary with temperature and to depend on the axial ligand. The results indicate that the fluoro-substituted porphyrins are primarily A_{2u} at low temperature, even though their room temperature spectroscopic features resemble those of A_{1u} cations. The elucidation of factors that affect the electronic structures of the radicals in the present series is helpful in providing a greater understanding of the spin–spin interactions in the intermediates of heme-dependant enzymatic reactions and their synthetic analogues.

Keywords
electronic structure · frontier orbitals · metalloporphyrins · radical cations

Introduction

Porphyrin radical cations play a crucial role in the various biological systems in which metalloporphyrins are involved.[1, 5–7] The interactions of metalloporphyrin radical cations with the central metal are expected to be sensitive to various factors, such as the substituents on the porphyrin, the characteristics of the metal and its ligands, and the symmetry of the complex.[2b, 3] Indeed, despite the similarity of the prosthetic group (hemin) in CAT, HRP, CCP, and P-450, their two-electron oxidation products (compounds I) are significantly different.[4] In all these cases, one electron is removed from the iron(III), forming an oxoiron(IV) center, while the second electron is usually removed from the porphyrin. The difference between them lies in the interaction between the oxoiron(IV) and the porphyrin radical cation. In HRP this interaction is exceedingly weak,[5] while in chloroperoxidase it is antiferromagnetic and moderately strong.[6] In the case of CCP, an amino acid and not the porphyrin is oxidized,[7] and compound I of P-450 remains elusive. Porphyrin radical cations are also extensively studied in synthetic systems with the aim of understanding their interactions with paramagnetic metals.[8] In two such compounds, the spin–spin interactions are again quite different. For example, in the extensively studied model compound, oxoiron(IV) tetramesitylporphyrin radical cation, the interaction of the radical cation with the oxoiron(IV) moiety is strongly ferromagnetic, dissimilar to any known compound I of an enzyme.[9] Meanwhile, the porphyrin radical–oxoiron(IV) interaction is again different for a very similar compound, oxoiron(IV) tetra(2,6-dichlorophenyl)porphyrin radical cation.[10] One variable that might affect the coupling between the metal electrons and the porphyrin radical is the identity of the magnetic orbital in the latter.

The metalloporphyrin frontier molecular orbitals, as described by the four orbital model,[11] were identified as a set of degenerate LUMOs ($4e_g$) and two closely spaced HOMOs ($1a_{1u}$ and $3a_{2u}$ in D_{4h} symmetry).[12] Upon oxidation of a porphyrin to its radical cation, the a_{1u} or the a_{2u} orbital becomes the magnetic orbital, leaving an A_{1u} or A_{2u} ground state and a low-lying A_{2u} or A_{1u} excited state, respectively. These states are allowed to mix through a pseudo-Jahn–Teller distortion along A_{2g} modes in the idealized D_{4h} symmetry.[13]

To focus on the effects that substitutents exert on the HOMO of the porphyrin cation, simpler synthetic systems are necessary. For zinc(II) and magnesium(II) porphyrin radical cations the two types of radicals were observed experimentally. Their unambiguous identification was based on spectroscopic distinctions due to the very different spin distribution in the a_{1u} and a_{2u} orbitals (Fig. 1). In [(OEP$^{\cdot+}$)Mg] (**1**, all β-pyrrole positions sub-

[*] Dr. Z. Gross, M. S.-Chem. C. M. Barzilay
Department of Chemistry, Technion—Israel Institute of Technology
Technion City, Haifa 32000 (Israel)
Telefax: Int. code + (972)4233-735
e-mail: chr10zg@technion.technion.ac.il
Prof. T. G. Spiro, S. A. Sibilia
Department of Chemistry, Princeton University
Princeton, NJ 08544 (USA)

0570-0833/95/0404-0222 $ 40.00+.25/0

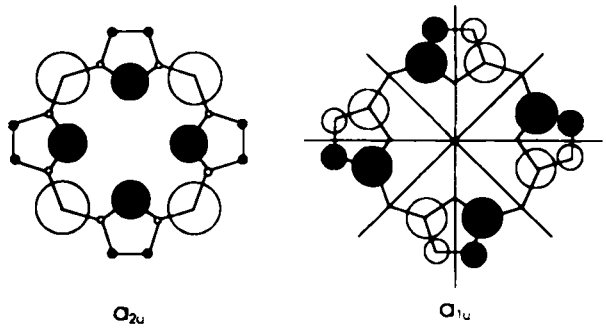

Fig. 1. Schematic presentation of the two highest occupied molecular orbitals of the D_{4h} porphyrin ring, reproduced from ref. [3c]. The sizes of the circles are proportional to the square of the orbital coefficients at each atom, where filled and empty circles represent negative and positive coefficients, respectively.

stituted) the single electron was shown to be located in an a_{1u} orbital, whereas the *meso*-phenyl-substituted complex, [(TPP$^{+\cdot}$)Mg] (**2**), showed spectral features indicative of an A_{2u} ground state.[14] The similarities of the electronic spectra of **1** and **2** to that of [(OEP$^{+\cdot}$)Co^{III}Br$_2$] and [(OEP$^{+\cdot}$)Co^{III}(ClO$_4$)$_2$], respectively, which in turn resembled the spectra of compounds I of CAT and HRP, respectively, were considered as evidence for different ground states in the porphyrin radical of the two enzymes.[15] But, during the last two decades many contradictory results were obtained regarding the relative order of the two highest occupied orbitals in porphyrin-oxidized metallooctaethylporphyrins, and reports of spin-admixed ground states have appeared recently.[16] Since the electronic spectral characteristics was sometimes not in accord with other spectroscopic evidence, the UV/Vis criterion for assignment of the electronic state of metalloporphyrin radicals containing transition metals was generally considered not to be valid.[16, 17]

Because of the large structural differences between OEP and TPP there is an increasing interest in observing both type of radicals for TPP derivatives. Until very recently, all metallotetraarylporphyrin radical cations (TPP derivatives) were considered to have A_{2u} ground states with little or no contribution of the A_{1u} state.[16a, 17] Some recent calculations were performed to examine the influence of phenyl-ring substituents on the a_{1u} and a_{2u} orbitals of TPP derivatives (tetraarylporphyrins), but the relative order of the orbitals was not elucidated.[18, 2c]

In preliminary studies we isolated two new tetraarylporphyrin radical cations and showed that the substitution of phenyl ring hydrogens in TPP by electron-withdrawing groups resulted in the first example of A_{1u} tetraarylporphyrin radical cations, in which the β-pyrrole hydrogens are not substituted.[19] We have now prepared an extensive series of halogen-substituted Mg and Zn porphyrin cations and studied their spectroscopic features at various temperatures by means of ESR, UV/Vis, and resonance Raman spectroscopy. The porphyrins were selected to determine the interplay between the type and position of the substituent and its effect on the porphyrin ring. Low-temperature measurements were obtained to determine the temperature dependence of the UV/Vis and ESR measurements and to compare these results with those obtained by resonance Raman spectroscopy. In addition, the effect of coordinating axial ligands was studied. These results shed new light on how substitutents affect the electronic structures of porphyrin radical cations, which might support a more fundamental understanding of the various modes of intramolecular interactions between the central metal and porphyrin radicals.

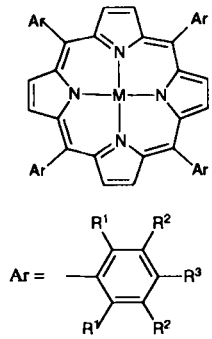

Neutral Species						Radical Salts	
No.	R^1	R^2	R^3	Abbreviation	M	No.	Salt
3	H	H	H	TPP	Zn	**3a**	[$3^{+\cdot}$]$SbCl_6^-$
4	CH_3	H	CH_3	TMP	Zn	**4a**	[$4^{+\cdot}$]$SbCl_6^-$
5	H	Cl	H	T*m*-dClPP	Zn	**5a**	[$5^{+\cdot}$]$SbCl_6^-$
6	Cl	H	H	T*o*-dClPP	Zn	**6a**	[$6^{+\cdot}$]$SbCl_6^-$
7	F	F	F	TpFPP	Zn	**7a**	[$7^{+\cdot}$]$SbCl_6^-$
8	F	F	F	TpFPP	Mg	**8a**	[$8^{+\cdot}$]$SbCl_6^-$
9	F	H	H	T*o*-dFPP	Zn	**9a**	[$9^{+\cdot}$]$SbCl_6^-$
10	F	H	H	T*o*-dFPP	Mg	**10a**	[$10^{+\cdot}$]$SbCl_6^-$

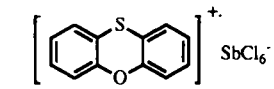

11a

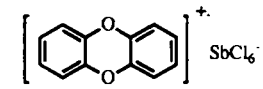

12a

Experimental Section

Solvents: CH_2Cl_2 (HPLC grade, Labscan) was dried by distillation over CaH_2, and THF (Riedel de Haën) by distillation over potassium and benzophenone. CD_2Cl_2 (Aldrich), $CDCl_3$ (Aldrich) and CH_3OH (absolute) were used as received.

Zn and Mg Porphyrins: The required porphyrins were prepared and metalated by routine methods [20]. The zinc(II) porphyrins (**3**–**7**, **9**) are known and were characterized by UV/Vis spectroscopy and ^{19}F and ^{1}H NMR [21]. The magnesiun(II) complexes **8** and **10** were prepared by refluxing the corresponding porphyrins in DMF with magnesium chloride (8 and 12 h, respectively) [20b], followed by chromatography (neutral silica; hexanes/CH_2Cl_2; 1:1 for elution of unreacted porphyrin and 1:4 and 2:3 for isolation of **8** and **10**, respectively) and recrystallization from CH_2Cl_2/hexanes mixtures. Their characterization was based on MS and comparison of their ^{1}H NMR (200 MHz, referenced against residual $CHCl_3$ at $\delta = 7.259$), ^{19}F NMR (188 MHz, referenced against TFA at $\delta = -77$), and UV/Vis spectra with that of the corresponding zinc(II) complexes. Special care was taken during the chromatography of compounds **7** and **8**, because they were seriously contaminated by similar compounds in which the phenyl *p*-fluorides were partially replaced by dimethylamino groups (appearing at $\delta = 3.3$ in the ^{1}H NMR spectra) [22]. [(T*o*-dFPP)Mg] (**8**): UV/Vis (CH_2Cl_2): λ_{max}/nm 420 (Soret), 558 (Q band); FAB MS (EI, *m*/*z*): 780.2 (M^+, 100%); ^{1}H NMR ($CDCl_3$): $\delta = 8.89$ (s, 8H), 7.76 (tt, $J_1 = 13.6$ Hz, $J_2 = 8.8$ Hz, 4H), 7.37 (m, 8H); ^{19}F NMR ($CDCl_3$): $\delta = -137.6$ (m, 8F). [(TpFPP)Mg] (**10**): UV/Vis (CH_2Cl_2): λ_{max}/nm = 420 (Soret), 556 (Q band); FAB MS (EI, *m*/*z*): 996.1 (M^+, 100%); ^{1}H NMR ($CDCl_3$): $\delta = 8.91$ (s, 8H). ^{19}F NMR ($CDCl_3$): $\delta = -138.0$ (dd, $J_1 = 23$ Hz, $J_2 = 7$ Hz, 8F), -153.1 (t, $J = 20.5$ Hz, 4F), -162.9 (m, 8F).

Radical Cations of Phenoxathiin and Dibenzo-1,4-dioxin: The radical cation of phenoxathiin (**11**) was prepared by the literature procedure [23], and **12a** was prepared in a similar fashion. Excess $SbCl_5$ was added to a stirred solution of dibenzo-1,4-dioxin [24a] (**12**) in CH_2Cl_2 under Ar. The blue solid, which separated almost immediately, was filtered and washed with $CHCl_3$. In the solid state it was stable for weeks. The ESR spectrum of **12a** showed a hyperfine structure (5 lines due to 4

Abstract in Hebrew:

תקציר: סדרה של מגנזיום ואבץ טטרהארילפורפירינים (**3** - **10**) ושל תוצרי החמצון הכימי שלהם (**3a** - **10a**) נחקרו במגוון טמפרטורות באמצעות ספקטרוסקופיה אלקטרונית, תהודת ספין-גרעין ותהודת רמן. למרות הדימיון המבני של כל הקומפלקסים, מצבי היסוד האלקטרוניים משתנים בתוך הסדרה. הרדיקלים **3a**, **4a** ונגזרת המטה-דיכלורו (**5a**) התאפינו בתכונות ספקטרוסקופיות של $A_{2\mu}$, הנגזרת האורתו-דיכלורו (**6a**) הראתה תכונות של $A_{1\mu}$, והרדיקלים של הפורפירינים המותמרי פלואור, במיוחד **10a**, נמצאו בעלי מבנים של מעורבי מצב אלקטרוני (A_{2u}/A_{1u}). התרומה היחסית של שני המצבים השתנתה כפונקציה של הטמפרטורה והיתה תלויה בליגנדה האקסיאלית. גלוי הגורמים המשפיעים על המבנים האלקטרוניים של הרדיקלים בסדרה הנוכחית תורם להגברת ההבנה של האינטראקציות ספין-ספין בחומרי הביניים בתגובות של המו-אנזימים והאנלוגים הסינתטיים שלהם.

equivalent H's and additional ^{13}C couplings) identical to literature reports [24b]. $\lambda_{max}(CH_2Cl_2) = 688$ nm. Anal. calcd. for $C_{12}H_8Cl_6O_2Sb$: C, 27.79; H, 1.56. Found: C, 27.86; H, 1.63.

Zn and Mg Porphyrin Radical Cations 3a–10a: The Zn and Mg porphyrin radical cations **3a–10a** were prepared by dissolving the corresponding metalloporphyrin (**3–10**) in CH_2Cl_2 under Ar, followed by addition of less than equimolar amounts of solid **11a** or **12a** (for **7a–9a**). After a few minutes, cold heptane was added to precipitate the oxidized metalloporphyrins. The green-black solids were isolated and purified by repeated centrifugation with heptane until no nonoxidized metalloporphyrins appeared in the electronic spectrum. The identification of the compounds was based on the well-known characteristics of porphyrin radical cations, such as **3a** [14, 25]. These are the blue-shifted and diminished intensity Soret bands and the appearances of new visible bands in the electronic spectra, as well as the appearances of ESR signals as outlined in detail in the text and in Figures 2–4.

ESR Spectroscopy: Samples for ESR spectroscopy were prepared by putting either the isolated metalloporphyrin radicals or solid metalloporphyrin together with about 0.5 equiv of **11a** or **12a** in a quartz ESR cuvette and degassing by vacuum. Dry and degassed CH_2Cl_2 was added by vacuum transfer into the liquid nitrogen cooled ESR tube. The tube was sealed and kept frozen until used for measurements. Spectra were obtained on a X-band E 4 Varian spectrometer at a microwave power of 5 mW. The g values (± 0.0005, referenced against $g = 2.0037$ for powdered DPPH) in CH_2Cl_2 at room temperature of **3a**, **4a**, **5a**, **6a**, **7a**, **8a**, **9a**, and **10a** were 2.0027, 2.0031, 2.0048, 2.0010, 2.0041, 2.0037 (2.0039 in 5% THF), 2.0034, and 2.0035 (2.0037 in 5% THF), respectively.

Electronic Spectra were obtained on a HP 8452A diode array spectrophotometer. The low temperature spectra were obtained with the aid of a homemade low T cell. The UV/Vis spectral characteristics of the radicals in CH_2Cl_2 (λ_{max}/nm) at room temperature were as follows: **3a**: 410 (Soret), no additional λ_{max}. **4a**: 412 (Soret), no additional λ_{max}. **5a**: 412 (Soret), no additional λ_{max}. **6a**: 371 (sh), 392, 410, 692. **7a**: 367 (sh), 386, 410, 682. **8a**: 367 (sh), 386, 406, 698. **9a**: 368 (sh), 386, 408, 688. **10a**: 368, 384, 406, 698.

Electrochemistry: The electrochemical oxidation potentials of the substituted porphyrins were determined by cyclic voltammetry (CV) at ambient temperatures on a homemade voltammograph, with CH_2Cl_2 solutions, 0.1 M in *n*-tetrabutylammonium perchlorate (Fluka, recrystallized three times from absolute ethanol) and 10^{-3} M in **3–12**. The reference electrode was SCE, the scan rate 100 mV sec^{-1}, and the $E_{1/2}$ value for oxidation of ferrocene under these conditions was 0.465 V. The $E_{1/2}$ values for the first oxidation of **3–12** are summarized in Table 1. Bulk electrolysis of compounds **3–10** at voltages 100 mV higher than their $E_{1/2}$ values were performed at 10^{-5} M substrate concentration. Their UV/Vis spectra were examined and found to be identical to the chemical oxidation products **3a–10a**.

Resonance Raman Spectroscopy: Room temperature measurements of the neutral porphyrins were obtained in 1 mM CH_2Cl_2 solutions of the porphyrin, except in the case of [(T*m*-dClPP)Zn] (**5**), whose solubility in CH_2Cl_2 was very low. The radical cations for these measurements were prepared under inert atmosphere (N_2, Airco Products, low O_2) in a Vacuum Atmospheres DL-001-SD Dri Lab, equipped with a HC-493 Dri-Train. The neutral porphyrin was dissolved in a minimal amount of CH_2Cl_2 in a test tube, equipped with a stir flea (Aldrich). An equimolar amount of oxidant was added and the solution was stirred until the absoption spectrum showed only the spectrum of the radical cation. The green-black solid was precipitated by the addition of hexanes (or heptane) to the test tube, after which the supernatant was withdrawn by a pipette. The solid was washed twice more with hexanes, dried, and redissolved in CH_2Cl_2. The absorption spectrum was rechecked as the Raman cell was loaded. Measurements of the electronic spectra during the glove-box operations were obtained through a fiber-optic attachment, connected to a HP 8451A diode array spectrophotometer.

The apparatus used for rR (resonance Raman) data collection consisted of a 1 cm diameter cylindrical cell, fitted with a spinfin (LabGlass) or a stir flea (Aldrich) magnetic stirring bar. The bottom part of the cell was approximately 6 cm long. The cell top, attached through an O-ring joint, allowed for evacuation of the cell and included a thermocouple port. Low temperatures used in the experiments were obtained by passing N_2, cooled through a copper tube immersed in liquid N_2, over the sample, which fitted into a glass dewar [26]. Resonance Raman spectroscopy was performed in the 135° backscattering geometry using a SPEX monochromater with a cooled RCA 31034A photomultiplier tube. Excitation wavelengths were obtained from a Coherent Innova 100 Kr^+ laser and a Liconix 4240PS HeCd laser. Data were collected for 1 s integrations at 1 cm^{-1} steps at 4 cm^{-1} slit widths. The data of the radical cations and the neutral porphyrins were collected at approximately -60 °C, and two scans were collected and averaged.

Results

Electrochemical Oxidation of the Metalloporphyrins, 3–10: The oxidation potentials ($E_{1/2}$) of the substituted Zn^{II} and Mg^{II} porphyrins were determined by cyclic voltammetry (CV) and are summarized in Table 1. The $E_{1/2}$ values of the halogen-substituted porphyrins became more positive in the order [(T*m*-dClPP)Zn] (**5**) = [(T*o*-dFPP)Mg] (**10**) < [(T*o*-dClPP)Zn] (**6**) < [(T*o*-dFPP)Zn] (**9**) < [(TpFPP)Mg] (**8**) < [(TpFPP)Zn] (**7**). It is noteworthy that the positive shift of the first oxidation potential of the porphyrin by *meta*-dichloro substitution in **5** relative to [(TPP)Zn] was 80 mV, while *ortho*-dichloro substitution in **6** caused a shift of 190 mV. The different type of substitution, F vs. Cl, in the *ortho*-positions had a similar effect on the oxidation potential; the [(T*o*-dFPP)Zn] (**9**) oxidation potential was only 20 mV more positive than that of [(T*o*-dClPP)Zn] (**6**). As expected, when the number of electron-withdrawing substituents increased, the effect on the oxidation potential increased too. Thus, for the pentafluorophenylporphyrin [(TpFPP)M] derivatives, the most positive oxidation potentials were observed. The metal ion also influenced the oxidation potential. The oxidation potentials of the Mg^{II} porphyrins were less positive than those of the Zn^{II} porphyrins for any given substitution pattern on the phenyl rings. Bulk electrolysis of metalloporphyrins **3–10** were performed at 10^{-5} M substrate concentration, at potentials which were higher than their $E_{1/2}$ values by 100 mV. Their UV/Vis spectra were examined and found to be identical to the chemical oxidation products (**3a–10a**).

Table 1. Half-wave oxidation potentials ($E_{1/2}$) of metalloporphyrins **3–10**, phenoxathiin (**11**), and dibenzo-1,4-dioxin (**12**) [a].

Substrate	$E_{1/2}$ (V)	Substrate	$E_{1/2}$ (V)
3	0.78 [b]	**9**	0.99 [c]
4	0.68	**10**	0.86
5	0.86	**11**	1.27
6	0.97 [c]	**12**	1.41
7	1.15 [c]		

[a] In CH_2Cl_2, 0.1 M in *n*-tetrabutylammonium perchlorate and 10^{-3} M in substrate, vs. SCE ($E_{1/2}$ of ferrocene under the same conditions was 0.465 V). [b] K. M. Kadish, L. R. Shiue, R. K. Rhodes, L. A. Bottomley, *Inorg. Chem.* **1981**, *20*, 1274–1277. [c] Very similar values were obtained by J. P. Collman et al. in ref. [21b].

Isolation of the Porphyrin Radical Cations 3a–10a: The radicals **3a–10a** were prepared by the chemical oxidation of **3–10**, respectively, with **11a**. The oxidation of **7–9** by **11a** was only partially complete even with an excess of the oxidant, most probably because of the very positive oxidation potentials of these derivatives (Table 1). Much better results were obtained by using **12a**, the radical cation of dibenzo-1,4-dioxin ($E_{1/2}$ of **12** = 1.41 V vs. SCE), which is a much more powerful oxidant than **11a** ($E_{1/2}$ of **11** = 1.27 V vs. SCE). The radical cations **3a–10a** were isolated as green-black solids. They were found to be stable for weeks in the solid state and no fast decomposition was observed in degassed $CHCl_3$ or CH_2Cl_2 solutions, where they appeared green, as expected for porphyrin radical cations. Addition of nBu$_4$NI regenerated the unoxidized precursors; the possibility of irreversible oxidation to isoporphyrins was thus eliminated.[27] By all spectroscopic criteria (UV/Vis, IR,[19] and ESR) the oxidation product of [(TPP)Zn] (**3a**) was identical to that of the oxidized species with a perchlorate counter ion ([**3**$^{\bullet+}$]ClO_4^-), which was reported earlier.[25] All the other products also had the spectroscopic characteristics of porphyrin radical cations as outlined in the following sections.

Electronic Spectra of 3a–10a at Various Temperatures: The UV/Vis spectra of radicals **3a–10a** were recorded at room temperature and compared to their neutral precursors (**3–10**), as well as

© VCH Verlagsgesellschaft mbH, D-69451 Weinheim, 1995 0570-0833/95/0404-0224 $ 40.00+.25/0 Chem. Eur. J. 1995, 1, No. 4

to each other. The spectra of all the oxidized porphyrins were different from those of the neutral species in a manner characteristic for ring-oxidized porphyrins, including a blue-shifted near-UV (Soret) band with reduced intensity and new bands at the red end of the visible spectrum, the Q band region. But, only the spectra of **4a**[19] and **5a** (Fig. 2a) were similar to that of the well established A_{2u} radical **3a**.[25] Their spectral characteristics included a single blue-shifted Soret band of low intensity relative to neutral porphyrins and several quite diffuse and characterless bands at the red end of the visible spectrum, the Q bands. The spectra of **6a–10a** (Figs. 2b,c) were very different from those of **3a–5a**. In the Soret region of their spectra three clearly separated peaks were observed, all of them blue-shifted (relative to their neutral precursors) to a greater extent than the band in **3a–5a**. In addition, one pronounced peak with a clear λ_{max} was observed at 680–700 nm in their spectra. All these spectral features were previously found only for $OEP^{\bullet+}$ and similar compounds.[25, 28]

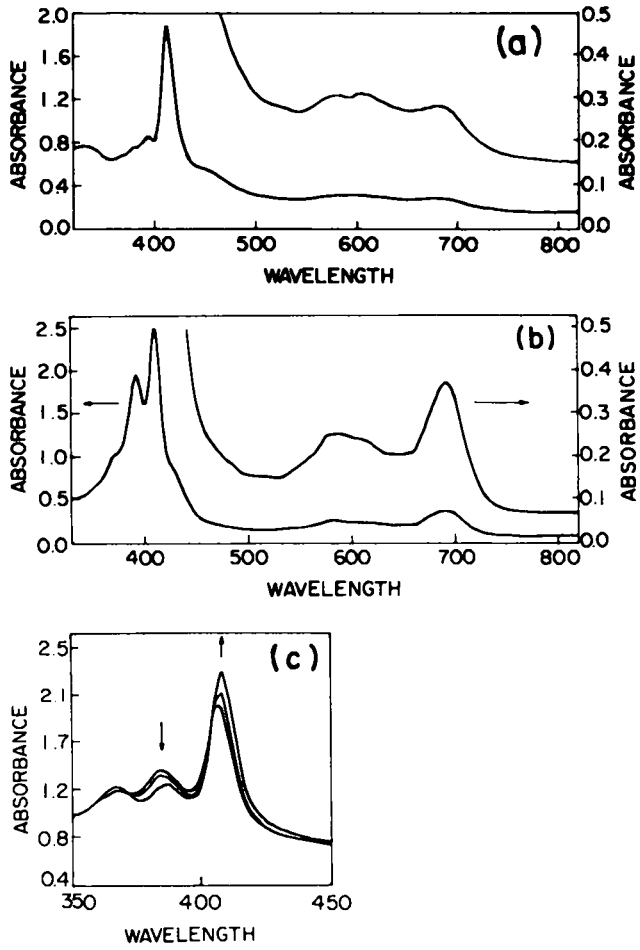

Fig. 2. Electronic spectra in CH_2Cl_2 at room temperature of (a) **5a**, (b) **6a**, and (c) **10a**. The arrows in (c) indicate the direction of the spectral changes that occurred upon lowering the temperature from 23 to 0 °C and to −40 °C.

The electronic spectra of radicals **6a–10a** were also examined as a function of temperature (25 to −90 °C). Remarkable changes were noticed in the Soret region of their spectra, most significantly for **10a** (Fig. 2c). As the temperature was lowered, the lowest energy absorption band increased in intensity and shifted to the red (406 → 410 nm), while the peak next to it, in addition to its red shift (384 → 388 nm), also lost intensity. For the radicals **7a–9a** similar changes in the Soret bands were noticed, but they were more moderate. With respect to the Q bands, red shifts of about 4–6 nm were obtained for radicals **7a–9a**, but the shape of the peaks were not affected by temperature. All these changes were completely reversible, the spectrum taken at high temperature was fully preserved after a cooling–warming cycle. In contrast to the other halide-substituted radicals, the electronic spectrum of **6a** was exceptionally unaffected by temperature changes in both its Soret and Q bands. Finally, the spectrum of **10a** in the presence of 5% CH_3OH or THF in CH_2Cl_2 at room temperature was identical to its spectrum at low temperature in the absence of these additives.

ESR Spectra of 3a–10a at Various Temperatures: The room temperature ESR spectra were obtained for all the radicals of the present study. Only the spectra of **3a–5a** (Fig. 3, traces a–c) showed a nine-line ESR spectrum (hyperfine coupling constant of 1.46, 1.75, and 1.56 G, respectively), characteristic for A_{2u} radicals.[14, 27] In contrast, singlets without hyperfine splittings were obtained under the same conditions for **6a–10a** (Fig. 3, traces d and e). Among these radicals the singlet of **6a** (trace d) was much sharper, with a peak-to-peak width (ΔH_{pp}) of 3.0 G, than that of the remaining compounds, which had a ΔH_{pp} of 4.2–5.1 G, and especially that of **8a**, which had a ΔH_{pp} of 6.75 G (trace e).[29]

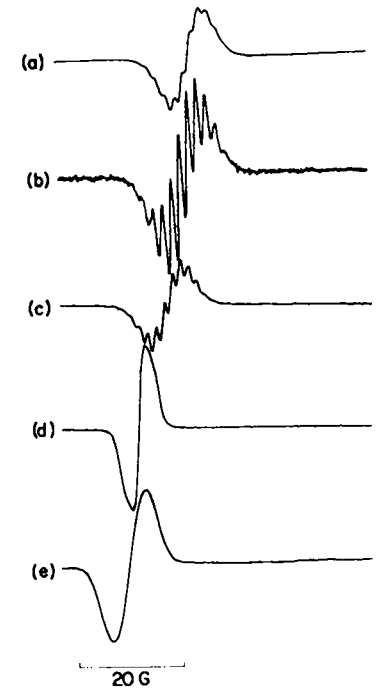

Fig. 3. ESR spectra in CH_2Cl_2 at room temperature of (a) **3a**, (b) **4a**, (c) **5a**, (d) **6a**, and (e) **8a**.

The spectra of radicals **6a–10a** were examined further in CH_2Cl_2 solutions in the temperature range between 25 and −90 °C. For **6a**, a relatively sharp singlet was observed at all temperatures. With ΔH_{pp} = 2.6 G at −90 °C, this derivative had the smallest linewidth of all radicals studied. For compounds **7a–9a** the linewidth changed only slightly (±5%) as the temperature was lowered. Much more significant changes were observed in the spectrum of **10a** (Fig. 4). As the temperature was gradually lowered, first the singlet broadened, but at −50 to −90 °C it was clearly split into a nine-line spectrum with hyperfine splitting constants of between 1.06 (−50 °C) and 1.10 G (−90 °C). The ΔH_{pp} of the singlet at 25 °C was 4.18 G, while the difference between the two highest peaks at −90 °C was 4.95 G. Radicals **8a**, **9a**, and **10a** were also examined in solutions that contained 5% MeOH or THF (by volume). This had no effect on the lineshape or -width of **8a** and **9a**, but for radical **10a** a nine-line spectrum (Fig. 4c) was obtained at all temperatures with hyperfine splitting constants of 1.17±0.04 G (slightly temperature dependent).

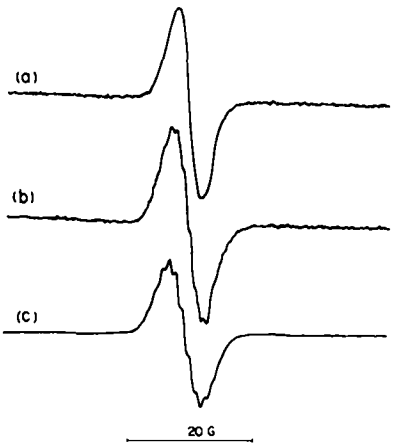

Fig. 4. ESR spectra of **10a** in CH_2Cl_2 at (a) 25 °C, (b) −90 °C, and (c) 25 °C in the presence of 5% methanol.

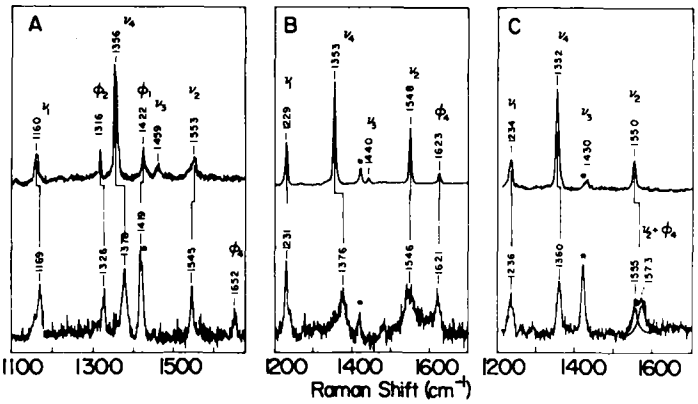

Fig. 5. Resonance Raman spectra of the neutral (top) and chemically oxidized (bottom) porphyrins at −60−−65 °C: A) **8** and **8a**, excitation wavelength = 406.7 nm; B) **10** and **10a**, excitation wavelength = 441.6 nm; C) **6** and **6a**, excitation wavelength = 441.6 nm (for the analysis, i.e., the curve fit, of ν_2 and ϕ_4 in this case, see text). Spectra were obtained with 50 mW laser power and 4 cm^{-1} slit widths. Asterisks indicate CH_2Cl_2 solvent bands.

Resonance Raman Spectra: The resonance Raman spectra of the neutral substituted porphyrins **6**–**10** were obtained in CH_2Cl_2 solution at room temperature and at low temperature (−60 to −65 °C). Lowering the temperature did not affect the vibrational frequencies of the neutral porphyrins. In Figure 5, the spectra of [(TpFPP)Mg] (**8**), [(T*o*-dFPP)Mg] (**10**), and [(T*o*-dClPP)Zn] (**6**) are shown together with the spectra of their radical cations at low temperature. Spectra (not shown) were also obtained for [(T*o*-dFPP)Mg] (**10**) in CH_2Cl_2 with 5% CH_3OH and with 5% THF, in order to examine the effects of axial ligation on the porphyrin frequencies. The excitation wavelengths were chosen to maximize signals from the radical cations, while minimizing interference from any residual neutral species. Skeletal mode assignments were made by comparison of the spectra with those of [(TPP)Mg] and [(TPP)Zn],[30] and following the normal mode calculations of Li et. al,[31] while phenyl mode assignments were made by comparison (Table 2)

Table 2. Comparison of the phenyl modes in phenyl-substituted porphyrins with model compounds.

Mode [a]	ϕ_1 (ν_2)	ϕ_2 (ν_{13})	ϕ_3 (ν_{20})	ϕ_4 (ν_{8a})	Ref.
Biphenyl	– [b]	–	–	1580–1611	[36]
Biphenyl-f_{10}	1476	1303	1152	1661	[32], [34]
[(TPP)Ni]	3071	3070	3069	1599	[31]
[(T*o*-dFPP)Mg] (**10**)	–	–	–	1623	this work
[(TpFPP)Mg] (**8**)	1422	1316		1657	this work
[(TpFPP)Zn] (**9**)	1421	1313		1651	this work
toluene	–	–	–	1604	[37]
2,6-dichlorotoluene	–	–	–	1561	[33]
[(T*o*-dClPP)Zn] (**6**)	–	–	–	1564	this work [c]

[a] See ref. [31] for mode description. Designations in parentheses are the corresponding benzene mode assignments. [b] – = modes outside the frequency region of interest (800–1700 cm^{-1}). [c] Only observed in **6a**, see text.

with model compounds: decafluorobiphenyl,[32] *ortho*-dichlorotoluene, and other halogen-substituted benzenes.[33, 34] The effects of phenyl-ring substitution on the vibrational frequencies of the neutral metalloporphyrins are summarized in Table 3.

Effects of substitution on the spectra of the neutral species: In the the Soret-enhanced resonance Raman spectra of the substituted porphyrins (Fig. 5 top, Table 3), the totally symmetric A_{1g} porphyrin skeletal modes are dominant, as expected from A-term

Table 3. Resonance Raman frequencies (cm^{-1}) for metallotetraarylporphyrins and their shift upon radical cation formation (Δ) [a].

Assignment [b]	ν_2	ν_3	ν_4	ν_1	ϕ_4	ϕ_1	ϕ_2
[(TPP)Mg] [c]	1539		1348	1233	1592	–	–
Δ	−11		+20	0	−2		
[(T*o*-dFPP)Mg] (**10**)	1548	1440	1353	1229	1623	–	–
Δ	−2		+23	+2	−2		
[(TpFPP)Mg] (**8**)	1553	1459	1356	1160	1657 [d]	1422	1316
Δ	−8		+22	+9	−5	−5	
[(TPP)Zn] (**3**) [c]	1550		1354	1235	1594	–	–
Δ	−7		−12	0	−2		
[(T*o*-dClPP)Zn] (**6**)	1550	1430	1352	1234	[e]	–	–
Δ	+14 [f]		+8	+2	[f]		
[(T*o*-dFPP)Zn] (**9**) [g]	1554	1443	1359	1229	1624	–	–
[(TpFPP)Zn] (**7**) [g]	1555	–	1355	1157	1651	1421	1313

[a] Δ = ν(oxidized)−ν(neutral). [b] Ref. [13]. [c] Ref. [30]. [d] Observed with 356.4 nm excitation. [e] This mode was observed only in the radical cation. [f] ν_2 and ϕ_4 in the radical cation are coupled, resulting in a broad peak, which can be fitted to a curve with two peaks, at 1555 and 1573 cm^{-1}. The midpoint frequency of 1564 cm^{-1} is taken as the accidentally degenerate frequency for these two modes. [g] Radical cation was not stable under the experimental conditions; therefore, no Δ values can be presented.

scattering from a D_{4h} porphyrin.[35] In addition, several other polarized bands were observed in the spectra, which were attributed to phenyl modes. For a rigorous assignment of the porphyrin skeletal modes it is necessary to first identify the phenyl mode frequencies that occur in the same spectral region. Substitution of the phenyl hydrogens by halogens affects the phenyl-mode frequencies of the neutral porphyrins, especially the phenyl-substitutent stretching modes of the pentafluorophenyl porphyrins. In [(TpFPP)Mg] (**8**), the C–F stretching bands can be identified at 1422 cm^{-1} (overlapping with a depolarized band of the solvent, CH_2Cl_2) and 1316 cm^{-1} (Fig. 5A). These are labeled ϕ_1 and ϕ_2, corresponding to the phenyl C–H stretching modes in TPP. The frequency shift upon F vs. H substitution on the phenyl groups is very similar to that observed on moving from biphenyl and decafluorobiphenyl (Table 2).[36, 32] A third C–F stretch, ϕ_3, is expected near

0570-0833/95/0404-0226 $ 40.00+.25/0 Chem. Eur. J. 1995, 1, No. 4

1152 cm^{-1} and may overlap with the porphyrin–phenyl stretch, ν_1, seen at 1160 cm^{-1}. In the other compounds studied (except [(TpFPP)Zn], **7**) and in metallo TPPs, ν_1 is at a significantly higher frequency, at around 1230 cm^{-1}. It has significant $(CCH)_{Ph}$ bending character, and its low frequency in **7** and **8** is probably due to the loss of this character when all the phenyl H atoms are replaced by F. There is also a considerable shift in ϕ_4, the phenyl ring stretching mode, on substitution of the phenyl C–H by C–F. The value is just below 1600 cm^{-1} in many [(TPP)M] complexes (M = Mg, Zn, Cu, Ni, FeCl), but occurs at 1651 and 1657 cm^{-1} in **7** and **8**, respectively. This assignment is supported by the decafluorobiphenyl spectrum,[32] in which this mode is observed at 1661 cm^{-1}. The high frequency of ϕ_4 is believed to be caused by changes in the electronic distribution of the phenyl ring introduced by the F substitutents.[34] In [(T*o*-dFPP)Zn] (**9**) and [(T*o*-dFPP)Mg] (**10**), ϕ_4 is assigned to the band at 1623 cm^{-1}, consistent with a more moderate electronic effect from only two F substituents on the phenyl ring. Substitution of the phenyl hydrogens by Cl atoms is expected to cause a lowering of the ϕ_4 frequency since it is observed at 1566 cm^{-1} in 2,6-dichlorotoluene.[33] The frequency shift relative to the unsubstituted molecule (ϕ_4 = 1604 cm^{-1} in toluene and 1599 cm^{-1} in 1,2,3-trimethylbenzene)[37] is not due to the change in mass of the substituent, but originates from the decreased force constant of the C–Cl bond relative to that of the C–H bond.[38] For [(T*o*-dClPP)Zn] ϕ_4 is not observed, but is present in the radical cation spectrum (see below).

The ν_2 modes in the substituted porphyrins are shifted to higher frequencies relative to TPP, to a greater extent for the Mg than for the Zn porphyrins. In TPP, coupling with the phenyl mode, ϕ_4, decreases the ν_2 frequency. Due to the shifts of the phenyl-mode frequencies in the substituted porphyrins, the two modes mix less; this results in an apparent shift of the ν_2 mode to higher frequency. The enhancement of ν_3 relative to the other totally symmetric modes is weak, as in the spectra of the corresponding MTPPs. Its frequencies are 1430–1459 cm^{-1} in the substituted porphyrins, lower than the value expected for Zn and Mg complexes of TPP. Small changes are observed for ν_4 in the substituted porphyrins, including shifts to higher frequencies of 4–5 cm^{-1} for the *ortho*-difluorophenyl porphyrins (**9** and **10**) and 8 cm^{-1} for [(TpFPP)Mg] (**8**).

Axial ligation: Addition of 5% THF or CH_3OH to the CH_2Cl_2 solution of [(T*o*-dFPP)Mg] affected the skeletal modes by decreasing the frequencies by 6 cm^{-1} for ν_2, 3–4 cm^{-1} for ν_3, and 6–7 cm^{-1} for ν_4. The effect on ν_1 was small (2 cm^{-1}) and variable, shifting to lower and higher frequencies for CH_3OH and THF, respectively. A small shift to lower frequency of ϕ_4 occurred too (2 cm^{-1}). Shifts of the skeletal modes above 1440 cm^{-1} (ν_2 and ν_3) to lower frequencies are indicative of an increase in the core size of the porphyrin, brought about by coordination of axial ligands (CH_3OH or THF in the present case) to the metal ion. The change in the frequency of ν_4 is considered to be due to a change in the effective nuclear charge of the central metal.[39]

Radical cations: The resonance Raman spectra of Zn and Mg tetraphenylporphyrin radical cations are difficult to obtain, since they are susceptible to photoreduction.[30] In the present series, [(TpFPP$^{\bullet+}$)Zn] (**7a**) and [(T*o*-dFPP$^{\bullet+}$)Zn] (**9a**) were found to be particularly susceptible to reduction, probably due to their very high oxidation potentials. In addition, in the presence of 5% CH_3OH or THF, even the spectra of [(T*o*-dFPP$^{\bullet+}$)Mg] (**10a**) could not be obtained, because of partial reduction to the parent porphyrin upon addition of the coordinating solvent at room temperature. Since the spectrum of the neutral derivatives was more strongly enhanced than that of the radical cations, the presence of small amounts of neutral species hampered the observation of chemically generated radical cations with CH_3OH or THF as axial ligands. The radicals [(TpFPP$^{\bullet+}$)Mg] (**8a**), [(T*o*-dFPP$^{\bullet+}$)Mg] (**10a**), and [(T*o*-dClPP$^{\bullet+}$)Zn] (**6a**) could be examined since they remained stable throughout the experiments. Their resonance Raman spectra are presented together with their neutral species spectra in Figure 5.

In the phenyl-substituted porphyrin radical cations, ν_2 was found at lower frequencies relative to the neutral species for **8a** and **10a**, consistent with the shift expected for A_{2u} porphyrin radical cations.[13] In addition, the phenyl mode, ϕ_4, gained intensity relative to ν_2, and shifted slightly to lower frequencies. The −8 cm^{-1} shift of ν_2 in **8a** relative to its neutral precursor [((TpFPP)Mg], **8**) is similar in magnitude to that observed in [(TPP$^{\bullet+}$)Mg] relative to [(TPP)Mg] (−11 cm^{-1}, Table 3). A much smaller shift of −2 cm^{-1} is observed for ν_2 in **10a** relative to [(T*o*-dFPP)Mg] (**10**). In **6a**, a broad feature is observed in the 1550–1600 cm^{-1} region. This feature, centered at 1564 cm^{-1}, is attributed to two peaks, as observed in the curve fit in C (bottom) of Figure 5. Although the ϕ_4 phenyl mode of **6** was not enhanced, it is expected to occur at about 1560 cm^{-1}, by analogy to its frequency in *ortho*-dichlorotoluene. Since the intensity of this phenyl mode relative to ν_2 is expected to increase upon oxidation,[13] as in **8a** and **10a** (Fig. 5), this doublet is assigned to ϕ_4 and ν_2. The accidental degeneracy of these two modes splits them into two components of higher and lower frequency as observed in the curve fit in Figure 5. The shift to *higher* frequency of ν_2 in the cation, relative to the neutral species, is consistent with that expected for an A_{1u} porphyrin radical cation.[13] These results are in excellent agreement with the ESR and UV/Vis results for **6a**.

Discussion

The objective of this study was to determine the factors that affect the relative order of the two highest occupied molecular orbitals in TPP derivatives. This was accomplished by examining the oxidation products of magnesium and zinc tetraarylporphyrins by spectroscopic methods. Magnesium and zinc porphyrins are especially well suited for this purpose for several reasons: a) the site of oxidation is undoubtedly the porphyrin and not the metal; b) they are oxidized much more easily than other metalloporphyrins,[40] which permits the isolation of a relatively large series of phenyl ring substituted TPP radical cations; c) their observed electronic spectra are very well reproduced and understood by theory;[41a] and d) because of the absence of orbital interactions with the central metals, the interpretation of their ESR spectra is quite straightforward.

In preliminary studies, the large differences between the room temperature spectroscopic features of **3a** and **4a** on the one hand and those of **6a** and **8a** on the other permitted their assignment as A_{2u} and A_{1u} radicals, respectively.[19] In order to further elucidate the factors that determine the electronic states of phenyl-substituted tetraphenylporphyrin radical cations, we have extended our series by four additional derivatives and have also studied their resonance Raman spectra as an additional spectroscopic tool. The present series now also includes the *o*-F (**7a** and **8a**) and the *m*-Cl (**3a**) derivatives, whose specific role was to distinguish between possible modes of stabilization (or destabilization) of the two different electronic states by electronegative substituents. Low-temperature measurements and axial-ligand effects were studied in order to understand the role of mixing of the A_{2u} and A_{1u} states.

  0570-0833/95/0404-0227 $ 40.00+.25/0

ESR as Probe for the Electronic Ground States of the Radicals: The ESR spectra of metalloporphyrin radical cations, in which the metal is magnesium(II) or zinc(II), is the most straightforward spectroscopic method for studying their electronic structures.[14] The spectrum of **3a** is well known and was recorded for comparison only, since it is considered the typical A_{2u} spectrum of porphyrin radical cations. From the spin density distribution of an A_{2u} radical (Fig. 1), a broad nine-line ESR spectra is expected due to high unpaired spin densities at the four equivalent nitrogens and at the *meso* carbon atoms from which it "leaks" to the phenyl rings, whose protons cause the line broadening.[25b] As shown in traces a–c of Figure 3, compounds **3a**–**5a** satisfy this expectation and can thus safely been assigned as A_{2u} radicals. The spectral narrowing of the lines in the spectrum of **4a** relative to that of **3a** was also observed by Ichimora et. al. and is probably characteristic for tetra(bis-*ortho*-substituted-phenyl)porphyrins.[29] On the other hand, the observation of *singlets* in the ESR spectra of **6a**–**10a** (traces d and e of Fig. 3) indicates that the unpaired electron is in the a_{1u} orbital, for which both theory (Fig. 1) and experiment suggest high unpaired spin densities at the α- (mostly) and β-pyrrole carbons, but zero at the nitrogens or the *meso*-carbon atoms.[2c] The broadness of the signals might be due to unresolved splitting from hydrogens on the β-pyrrole carbons or, alternatively, a result of some mixing between the A_{1u} and A_{2u} states. Unfortunately, the ESR spectra of A_{1u} tetraarylporphyrin radical cations cannot be compared to that of any previously known A_{1u} radical, such as $OEP^{\bullet+}$, because of the absence of *meso*-protons in the former and absence of pyrrole protons in the latter. There is, however, a significant difference of the spectral linewidth within the series of radicals **6a**–**10a**. As can be seen in Figure 3, the signal of **6a** (trace d) was much sharper than that of **8a** (trace e)[29] and of the singlets of the remaining compounds. In order to elucidate the origin of the broadening of the singlets, the ESR spectra of radicals **6a**–**10a** were examined in CH_2Cl_2 solutions at the temperature range between 25 and −90 °C and for **9a** and **10a** also in solutions that contained 5% CH_3OH or THF.

The temperature effect on the ESR spectra of the various radicals was very significantly different. For **6a**, a relatively sharp singlet with the smallest linewidth of all radicals studied was observed at all temperatures (ΔH_{pp} = 2.6 G at −90 °C), thus indicating one particular electronic ground state, namely, A_{1u} (ΔH_{pp} for [$(OEP^{\bullet+})$Zn] is about 3.5 G).[25b, 29b] For compounds **7a**–**9a** the linewidth was about two times broader (ΔH_{pp} = 4.6–5.1 G at −90 °C) than that of **6a**, which could be a result of some contribution of the A_{2u} state. The much more dramatic changes that were observed in the spectrum of **10a** (Fig. 4) served to clarify the situation. As the temperature was gradually lowered, first its singlet broadened, but between −50 and −90 °C hyperfine splitting into a nine-line spectrum was obtained. In the presence of CH_3OH or THF the hyperfine structure was obtained even at higher temperatures. Furthermore, the spectra of **10a** at −90 °C (Fig. 4b) and at 25 °C in solutions containing CH_3OH (or THF) (Fig. 4c) bear a remarkable similarity to those of **3a** and **5a** (Fig. 3a, 3c). The similar size of the hyperfine coupling constant (hfc) of **10a** (1.10–1.20 G) to that of **3a** (a_N = 1.46 G) and **5a** (a_N = 1.56 G), as well as the similarity of their coupling pattern, rules out the possibility that the hyperfine spectrum of **10a** is due to its eight β-pyrrole protons. (The multiplet due to 8 hydrogens ($I = {}^1/_2$) is very different from that of 4 nitrogens with I = 1.) In addition, the β-pyrrole hfc in the A_{2u} radicals [$(TTP^{\bullet+})$Zn] and [$(TPP^{\bullet+})$Zn] are only 0.036–0.072 G,[42] and since the spin density in A_{1u} radicals is only twice as high as in A_{2u} radicals, the predicted hfc of β-pyrrole protons in A_{1u} radicals is only 0.072–0.144 G. A much more reasonable explanation for the above-mentioned spectral changes is that they reflect changes in the electronic structure of **10a**. At high temperatures the spectra indicate predominant A_{1u} character, but at low temperatures or in the presence of methanol or THF a significant contribution of the A_{2u} state must be taken into account. This hypothesis was further checked by examination of the electronic spectra of the radicals.

Can the Electronic Spectra Be Used for Distinguishing between A_{2u} and A_{1u} Radicals? One of the earliest criteria introduced for porphyrin radical cations is their characteristic UV/Vis spectra.[43] It includes a blue-shifted near-UV (Soret) band with low intensity relative to neutral porphyrins and new bands at the red end of the visible spectrum. The two possible types of radicals, A_{1u} and A_{2u}, are further distinguished by the shape of the far-visible Q bands. In established A_{2u} radicals, such as **3a**, these bands are quite diffuse and characterless, whereas one pronounced λ_{max} is observed in the same spectral area for the prototype A_{1u} radical **1**.[25] But, several ($OEP^{\bullet+}$) derivatives, which according to this distinction were assigned as A_{2u} radicals, were found to be A_{1u} radicals by other spectroscopic methods.[16, 17] Quite recently,[17] an additional distinctive difference between the Soret bands of [$(TPP^{\bullet+})$Zn]ClO_4 (only one dominant band) and that of **1** (several bands) was related to the A_{2u} and A_{1u} states, respectively, based on theoretical arguments.[41a]

In Figure 2 the room temperature electronic spectra of **5a** (which is very similar to those of **3a** and **4a**)[19] and **6a** (representive of **7a**–**10a**) are compared. This comparison clearly shows that the characteristic Q bands of A_{2u} radicals[14, 17, 28] were observed only in the spectra of **3a**–**5a** (trace a), whereas the spectra of **6a**–**10a** (trace b) with the quite strong λ_{max} at 690–700 nm resembled A_{1u} radicals.[16] Close inspection of the near-UV part of the spectra disclosed additional significant differences. For **3a**–**5a** only one dominant band was observed, but for radicals **6a**–**10a** that spectral region was split into several bands. In summary, the room temperature electronic spectra of the radicals under study strongly indicates that only **3a**–**5a** are A_{2u} radicals, whereas **6a**–**10a** have spectral characteristics of A_{1u} radicals.

The variable-temperature UV/Vis spectra of radicals **6a**–**10a** were indicative of state mixing (A_{1u}/A_{2u}) in some of the radicals. The spectrum of **6a** was exceptionally unaffected by temperature changes, thus indicating that it remained an A_{1u} radical at all temperatures. In the radicals **7a**–**10a**, the Q bands were shifted to longer wavelengths (4–6 nm) without affecting their shape. Thus, according to the frequently used criteria (the shape of the Q bands), they should still be classified as A_{1u} radicals. The Soret part of their electronic spectra was, however, significantly altered as a function of temperature. The spectral changes were moderate for the radicals **7a**–**9a**, but quite pronounced for **10a** (Fig. 2c). As the temperature was lowered, the intensity of the main band at 406 nm increased and shifted to 410 nm, while that of the minor band at 384 nm decreased. As a result, the intensity ratio between the major band and the minor band was much higher at low than at high temperature. In addition, the spectrum of **10a** at −90 °C was indistinguishable from that of the same radical in a solution of 5% CH_3OH or THF in CH_2Cl_2 at 25 °C. Based on the above discussion of the sensitivity of the Soret bands to the electronic structure of the radicals (A_{2u} single Soret, A_{1u} split Soret), the spectral changes seem to reflect an increased weight of the A_{2u} state at lower temperatures or in the presence of CH_3OH (or THF). Although we do not claim to be able to quantify the spectral changes in terms of the amount of

0570-0833/95/0404-0228 $ 40.00+.25/0 Chem. Eur. J. 1995, 1, No. 4

state mixing,[17, 41] for the present purpose it is sufficient to state that the amount of contribution of the A_{2u} state to the electronic structures of the radicals is most significant for **10a**, less for **7a**–**9a**, and virtually absent for **6a**.

The most important observation of the variable-temperature studies is that identical results were obtained by ESR and UV/Vis spectroscopy. Thus, the spectra of **10a** are the most sensitive to temperature changes, **7a**–**9a** only moderately so, and both the ESR and the UV/Vis spectra of **6a** are essentially unaffected by variations in temperature. The spectroscopic results support the idea that the changes involved are due to changes in the relative contribution of the A_{1u} and A_{2u} states to the electronic configurations of the radicals at various temperatures. All the radicals **6a**–**10a** are predominantly A_{1u} at high temperatures, but with various contributions of A_{2u} at low temperatures: practically absent for **6a**, relatively high for **10a**, and intermediate for **7a**–**9a**.

RR Skeletal-Mode Frequency Shifts are Correctly Predicted by the ESR and UV/Vis Results: Among the various skeletal-mode frequency shifts in the resonance Raman spectra of the Mg^{II} and Zn^{II} phenyl-ring substituted TPP's and their radical cations that we have analyzed in this study, the most important one is the ν_2 vibration. This mode has been established as a marker band for determination of the HOMO in the porphyrin because of its shift upon oxidation ($\Delta\nu_2$).[13] The sensitivity of this mode, primarily a $C_\beta C_\beta$(C_β = β-pyrrole carbon) stretching mode, arises from the different atomic orbital coefficients of the $C_\beta C_\beta$ bond in the a_{2u} and a_{1u} orbitals (Fig. 1). Removal of an electron from the a_{2u} orbital, which is bonding about the $C_\beta C_\beta$ bond, decreases the bond order. This is reflected in a decrease (downshift) in the ν_2 frequency. In contrast, removal of an electron from the a_{1u} orbital results in a shift of ν_2 to higher frequency (upshift) upon oxidation, since $C_\beta C_\beta$ is antibonding in this orbital. This criterion for the identification of the electronic states of oxidized metalloporphyrins is consistent with the shifts for the A_{2u} radicals [(TPP$^{\bullet+}$)Zn] and [(TPP$^{\bullet+}$)Mg] ($\Delta\nu_2 = -7$ and $-11\ cm^{-1}$, respectively)[30] and for the A_{1u} radical [(OEP$^{\bullet+}$)Zn] ($\Delta\nu_2 = +19\ cm^{-1}$).[44] In the present series, $\Delta\nu_2 = -8\ cm^{-1}$ in [(TpF-PP$^{\bullet+}$)Mg] (**8a**), while $\Delta\nu_2 = -2\ cm^{-1}$ only for [(To-dF-PP$^{\bullet+}$)Mg] (**10a**), and $\Delta\nu_2 = +14\ cm^{-1}$ for [(To-dClPP$^{\bullet+}$)Zn] (**6a**) (Fig. 5, Table 3). Accordingly, the radicals **8a** and **6a** are assigned as A_{2u} and A_{1u} radicals, respectively. In an idealized D_{4h} symmetry, the two closely lying excited states of the cation are allowed to mix along A_{2g} vibrational coordinates through a pseudo-Jahn–Teller distortion.[13] The small shift in the ν_2 frequency in **10a** may be due to a large degree of mixing of its a_{1u} and a_{2u} orbitals. The opposite trends (upshift for A_{1u} and downshift for A_{2u} radicals) would tend to cancel the shift when mixing is strong. Mixing is supported by the ESR and UV/Vis data for **10a**.

Rationale for the Effects of Substituents, Temperature, and Axial Ligands on the Electronic Ground States: The present results show that the electronic configuration of the phenyl-substituted TPP radicals **5a**–**10a** are a function of the substituent and its position: 2,6-dichloro (**6a**) is A_{1u}, 3,5-dichloro (**5a**) is A_{2u}, and the 2,6-difluoro (**9a**, **10a**) are A_{1u}/A_{2u} spin-admixed. All three spectroscopic methods lead to the same conclusions for the radicals at the temperatures at which measurements were obtained. The pentafluoro-substituted radicals (**7a**, **8a**) are spin-admixed according to UV/Vis and ESR, but A_{2u} radicals by the rR criteria. The substituent effect on the oxidation potential of the porphyrins is 2,3,4,5,6-pentafluoro > 2,6-difluoro ≈ 2,6-dichloro > 3,5-dichloro (Table 1, $E_{1/2}$ of **7** > **9** ≈ **6** > **5**). This explicitly reflects the energy of the HOMO, but not its identity. Somewhat surprising is the similar effect of *ortho*-dichloro and *ortho*-difluoro substituents on the oxidation potentials, as well as the much lower effect of *meta*-dichloro substitution. The best way to accommodate these results is by separation of the polar (inductive), resonance, and steric effects of the substituents, related to Hammett constants.[45] The polar effects are described by σ^*, for the *ortho* substituents (σ^* = 0.37 (*o*-Cl) and 0.41 (*o*-F)), and σ_m = 0.37 (*m*-Cl); this results in an expected order of $E_{1/2}$ values of **9** > **6** = **5**. The resonance effects of the substituents are described by σ_R (σ_R = −0.35 (F) and −0.20 (Cl)). The stronger resonance parameter for F is reflected in the upshift of the ϕ_4 phenyl mode frequency in 2,6-difluoro, and especially pentafluoro, vs. the downshift observed for 2,6-dichloro. The resonance vs. inductive trends may also account for the similarity of the effects of *o*-F and *o*-Cl substituents on the oxidation potential of the porphyrin. The position of the Cl substituents in **5** mitigates their influence, even though the polar constant would indicate that an equal effect is expected for *o*- or *m*-Cl substitution.

The inductive effect in the pentafluorophenyl cations **7a** and **8a** is much larger than in the difluorophenyl cations **9a** and **10a**. That is the main reason for the high oxidation potentials of **7a** and **8a**. The A_{2u} ground state is probably a result of the additional *p*-F substituent, with its significant resonance contribution. The discrepancy between the ESR and the rR results for the pentafluoro derivatives might be due to a very large perturbation of the orbital coefficients of the atomic orbitals of the relevant porphyrin orbitals by these heavily substituted phenyls. This will have a significant effect on the hyperfine coupling constants in the ESR spectra of the radicals, which might result in broad unresolved signals. The direction (positive or negative) of the most important rR spectral shift, namely, the difference in ν_2 between the oxidized and the neutral derivative, is not affected by such perturbations, because it relies on the relative signs and not the absolute numbers of the coefficients on the two adjacent C_β carbons.

Although the polar and resonance effects of the substituents describe the changes in energy of the HOMO, the observed ordering of orbitals seems to originate from the steric inhibition (2,6-dichlorophenyl > 2,6-difluorophenyl > 3,5-dichlorophenyl) of interaction between the substituted phenyl ring and the porphyrin.[46] The major effect of the above-mentioned resonance interaction is a destabilization of the a_{2u} orbital energy. Because of the large coefficient in this orbital at the C_m position (Fig. 1), it is raised by the filled–filled orbital interactions with the phenyl ring. These arguments are in complete agreement with the fact that the radical **6a** has an A_{1u} ground state, **9a** is spin-admixed, and **5a** is an A_{2u} radical. In Scheme 1 these effects are presented pictorially. Situation *a* describes the orbital order expected based on the polar effect of the substituent alone, while

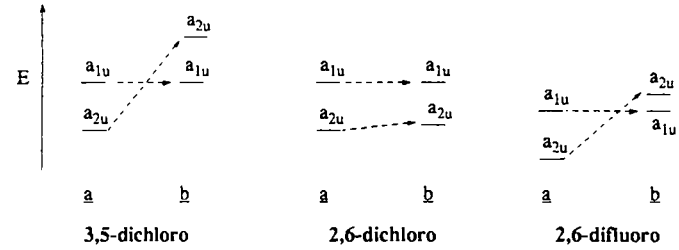

Scheme 1. Pictorial description of the effect of halogen substituents on the oxidation potential and on the relative energies of the two highest occupied MO's of phenyl-substituted tetraphenylporphyrinato zinc: a) considering only polar effects and b) including the resonance effect.

  0570-0833/95/0404-0229 $ 40.00+.25/0

in *b* the resonance interaction of the substituted phenyl ring with the porphyrin is taken into account. The energy of the a_{1u} orbital was left constant in the transformation of *a* to *b*, since, because of its nodal character at the phenyl ring carrying *meso* carbon, it is not expected to be affected by interaction of the porphyrin with the phenyl groups.

It must be emphasized that the above-mentioned steric effects are much more important for the oxidized derivatives than for their precursors. It is well known that the rotation of the phenyl groups in *ortho*-substituted tetraarylporphyrins is severely limited: it is quite fast for *o*-H, much slower for *o*-F, and completely blocked for *o*-Cl or larger substituents.[46] Crystallographic studies on porphyrin radical cations have shown that the porphyrin ring is usually not planar and that the dihedral angle between the phenyl groups and the porphyrin ring is much smaller (closer to coplanarity) than in the nonoxidized precursors.[47a] For example, the lowest phenyl dihedral angle in [(TPP)Zn] is 60.6°, but only 44.3° in [(TPP$^{\bullet+}$)Zn] and 42.1° in [(TPP$^{\bullet+}$)Mg].[48b-d] In this respect, in all the porphyrin radical cations that were investigated in the present study by rR, the phenyl ϕ_4 mode is enhanced to a much greater extent than in the neutral precursors. The resonance Raman intensity arises from displacements along the modes that are induced by the transition from the ground state to the excited state. This increase in intensity for the phenyl mode may be explained by the adoption of a nonplanar conformation of the porphyrin macrocycle, in either the ground or the excited state. As the molecule distorts from planarity, the interactions between the porphyrin and the phenyl rings increase, enabling delocalization of significant electron density onto the phenyl rings, as has been observed in the persubstituted porphyrins and in the persubstituted Zn *meso*-tetraphenyltetrabenzoporphyrin radical cation.[48] Nonetheless, the A_{1u} nature of **6a** remains evident, as observed in the upshift of the ν_2 marker band.

In Scheme 2, the effects of the substituents are summarized, showing the cumulative effect of the phenyl groups on the relative energies and orbital ordering of the porphyrin. The energy of the HOMO decreases along the series as indicated, governed mostly by inductive effects and reflected in the oxidation potentials. The orbital ordering is dominated by resonance effects, whose strengths determine whether the energy of the a_{2u} orbital will be well above (*o*-H), close to (*o*-F), or below (*o*-Cl) that of the a_{1u} radical.

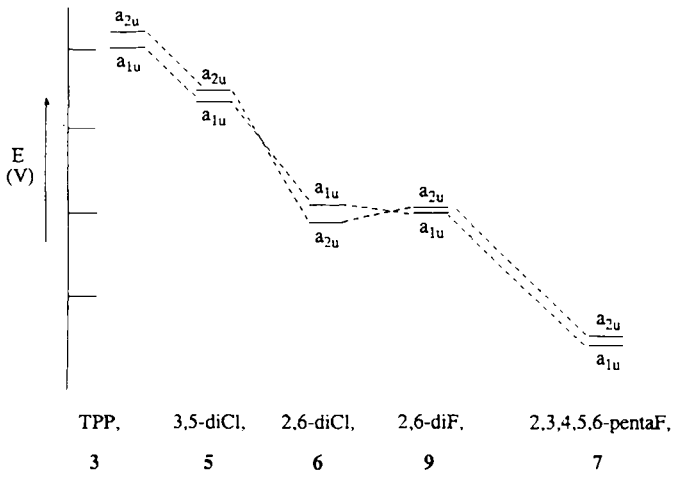

Scheme 2. The substituent effect on the energies of the two highest occupied molecular orbitals of tetraphenylporphyrin. The scale is based on the oxidation potentials of the Zn derivatives.

Finally, the effect of temperature and axial ligation on the spectral properties of **10a** are discussed. The fact that at low temperatures a nine-line ESR spectrum is observed and the UV/Vis spectrum changes toward "A_{2u}-like", suggests that its ground-state configuration is actually $(a_{1u})^2(a_{2u})^1$, with a very closely lying excited state of $(a_{1u})^1(a_{2u})^2$. As the temperature is lowered, the excited state configuration becomes less significantly occupied, which explains the spectral changes toward "A_{2u}-like" for **10a** at low temperatures.[49] Methanol and THF act as axial ligands toward the magnesium ion and push electrons into the empty p_z orbital. The symmetry in the resulting five-coordinate complex is the same as the a_{2u} orbital (a_1, C_{4v} symmetry), thus providing a mechanism (through the interaction of the filled p_z and the half-filled a_{2u} orbitals) for an additional promotion of this orbital above the a_{1u} orbital (a_2 in C_{4v} symmetry).[50] A very similar effect is probably responsible for the observation that for the oxoiron(IV) porphyrin radical cation with the same porphyrin as in **6a**, the magnetic orbital was found to be a_{2u}.[16a] Since in these complexes a strong intramolecular ferromagnetic interaction between the electrons of the metal and that of the porphyrin ($S' = {}^3/_2$ from $S = 1$ (Fe^{IV}) + $S = {}^1/_2$ ($P^{\bullet+}$)) is known to exist,[11] the porphyrin radical necessarily interacts with a metal orbital. The most suitable candidate is the filled d_{z^2} (or $(dp)_z$) orbital, which is part of the iron–oxygen σ bond and has the same symmetry as the a_{2u} orbital in C_{4v} symmetry (both are a_1) or lower. Again, because of the filled–half-filled orbital interaction, the a_{2u} orbital is raised in energy above the a_{1u} orbital, which has no matching metal orbital to interact with.

Conclusions

We have shown that the electronic configurations of tetraarylporphyrin radical cations are very sensitive to the remote phenyl-ring substituents. Only for large and electron-withdrawing substituents at the *ortho*-phenyl positions is a pure A_{1u} state possible. The electronic spectra of the radical cations must be examined with great care, since the "A_{1u}-like" spectrum is much more dominant than that of the "A_{2u}-like" spectrum. Accordingly, many radicals, including four of the present series, which have a "A_{1u}-like" spectrum are actually cases of spin-admixed states. Finally, the results suggest that the ability of different axial ligands to reverse the stability of the a_{2u} and a_{1u} orbitals by π-donation and/or geometry (symmetry) changes are responsible for the various modes of spin–spin interactions in heme-dependant enzymes and their synthetic models. This subject is currently under investigation in our groups.

Acknowledgment: This research was supported by the New York Metropolitan Research Fund, the Pollard Biochemical Engineering Research Fund, the Henri Gutwirth Fund for the Promotion of Research, and grant DE-FG02-93ER14403 (TGS) from the US Department of Energy. We also thank Prof. A. Halevi from the chemistry department at the Technion for helpful discussions.

Received: December 14, 1994 [F36]

[1] a) Y. Watanabe, J. T. Groves in *The Enzymes, Vol. 20* (Ed.: D. S. Sigman), Academic Press, California, **1992**, pp. 406–452. M. A. Ator, P. R. Ortiz de Montellano, *ibid. Vol. 19*, **1990**, pp. 214–282. b) L. A. Andersson, J. H. Dawson, *Structure and Bonding (Berlin)* **1991**, *74*, 1–40. c) *Cytochrome P-450: Structure, Mechanism and Biochemistry* (Ed.: P. R. Ortiz de Montellano), Plenum Press, NY, **1986**.

[2] More recent calculations and presentations as well as comprehensive discussions of that subject can be found in: a) R. A. Binstead, M. J. Crossley, N. S. Hush, *Inorg. Chem.* **1991**, *30*, 1259–1264. b) S. Nakashima, H. Ohya-Nishiguchi, N. Hirota, H. Fujii, I. Morishima, *Inorg. Chem.* **1990**, *29*, 5207–5211. c) A. G. Skillman, J. R. Collins, G. H. Loew, *J. Am. Chem. Soc.* **1992**, *114*, 9538–9544.

[3] P. Gans, G. Buisson, E. Duee, J.-C. Marchon, B. S. Erler, W. F. Scholz, C. A. Reed, *J. Am. Chem. Soc.* **1986**, *108*, 1223–1234.

[4] Abbreviations: OEP and TPP are the dianions of octaethyl- and of tetraphenylporphyrin respectively; $OEP^{\cdot+}$ and $TPP^{\cdot+}$ are one-electron oxidized OEP and TPP, respectively. CAT, HRP, CCP and P-450 are catalases, horseradish peroxidase, cytochrome C peroxidases, and cytochrome P-450, respectively.

[5] a) A. Gold, K. Jayaraj, P. Doppelt, R. Weiss, E. Bill, X.-Q. Ding, E. L. Bominaar, A. X. Trautwein, H. Winkler, *New J. Chem.* **1989**, *13*, 169–172. b) V. Roberts, B. M. Hoffman, R. Rutter, L. P. Hager, *J. Biol. Chem.* **1981**, *256*, 2118–2121.

[6] R. Rutter, L. P. Hager, H. Dhonau, M. Hendrick, M. Valentine, P. Debrunner, *Biochemistry* **1984**, *23*, 6809–6816.

[7] B. M. Hoffman, J. E. Roberts, C. H. Kang, E. Margoliash, *J. Biol. Chem.* **1981**, *256*, 6556–6564.

[8] a) A. X. Trautwein, E. Bill, E. L. Bominaar, H. Winkler, *Structure and Bonding (Berlin)* **1991**, *78*, 83–95. b) H. Fujii, *Inorg. Chem.* **1993**, *32*, 875–879. c) Y. Tokita, K. Yamaguchi, Y. Watanabe, I. Morishima, *Inorg. Chem.* **1993**, *32*, 329–333. d) H. Fujii, K. Ichikawa, *Inorg. Chem.* **1992**, *31*, 1110–12.

[9] a) J. T. Groves, R. C. Haushalter, M. Nakamura, T. E. Nemo, B. J. Evans, *J. Am. Chem. Soc.* **1981**, *103*, 2884–2886. b) E. Bill, X.-Q. Ding, E. L. Bominaar, A. X. Trautwein, H. Winkler, D. Mandon, R. Weiss, A. Gold, K. Jayaraj, W. E. Hatfield, M. L. Kirk, *Eur. J. Biochem.* **1990**, *188*, 665–672.

[10] Ref. [8a] and [9b], but see also: D. Mandon, R. Weiss, K. Jayaraj, A. Gold, J. Terner, E. Bill, A. X. Trautwein, *Inorg. Chem.* **1992**, *31*, 4404–4409.

[11] M. Gouterman in *The Porphyrins, Vol. 3* (Ed.: D. Dolphin), Academic Press, New York, **1979**, Chap. 1, p. 93.

[12] a) H. C. Longuet-Higgins, C. W. Rector, J. R. Platt, *J. Chem. Phys.* **1950**, *18*, 1174–1181. b) D. Spangler, G. M. Maggiora, L. L. Shipman, R. E. Christofferson, *J. Am. Chem. Soc.* **1977**, *99*, 7478–7489.

[13] R. S. Czernuszewicz, K. A. Macor, X.-Y. Li, J. R. Kincaid, T. G. Spiro, *J. Am. Chem. Soc.* **1989**, *111*, 3860–3869.

[14] J. Fajer, M. S. Davis, in *The Porphyrins, Vol. 4* (Ed.: D. Dolphin), Academic Press, New York, **1979**, Chap. 4.

[15] D. Dolphin, R. H. Felton, *Acc. Chem. Res.* **1974**, *7*, 26–32.

[16] a) M. Satoh, Y. Ohba, S. Yamauchi, M. Iwaizumi, *Inorg. Chem.* **1992**, *31*, 298–303 and references therein. b) W. R. Scheidt, H. Song, K. J. Haller, M. K. Safo, R. D. Orosz, C. A. Reed, P. G. Debrunner, C. E. Schulz, *Inorg. Chem.* **1992**, *31*, 939–941 and references therein.

[17] a) H. Fujii, *J. Am. Chem. Soc.* **1993**, *115*, 4641–4648. b) Z. Gasyna, M. J. Stillman, *Inorg. Chem.* **1990**, *29*, 5101–5109.

[18] P. G. Gassman, A. Ghosh, J. Almlof, *J. Am. Chem. Soc.* **1992**, *114*, 9990–10000.

[19] Z. Gross, C. Barzilay, *Angew. Chem.* **1992**, *104*, 1672–1674; *Angew. Chem. Int. Ed. Eng.* **1992**, *31*, 1615–1617.

[20] a) J. S. Lindsey, R. W. Wagner, *J. Org. Chem.* **1989**, *54*, 828–839. b) A. D. Adler, F. R. Longo, F. Kampas, J. Kim, *J. Inorg. Nucl. Chem.* **1970**, *32*, 2443–2445.

[21] a) K. Ichimori, H. Ohya-Nishiguchi, N. Hirota, *Bull. Chem. Soc. Jpn.* **1988**, *61*, 2753–2762. b) J. P. Collman, P. D. Hampton, J. I. Brauman, *J. Am. Chem. Soc.* **1990**, *112*, 2986–2998. c) S. Banfi, F. Montanari, S. Quici, *J. Org. Chem.* **1988**, *53*, 2863–2866.

[22] K. M. Kadish, C. Araullo-McAdams, B. C. Han, M. M. Franzen, *J. Am. Chem. Soc.* **1990**, *112*, 8364–8368.

[23] P. Gans, J.- C. Marchon, C. A. Reed, J. -R. Reynard, *Nouv. J. Chim.* **1981**, *5*, 203–204.

[24] a) H. Gilman, J. J. Dietrich, *J. Am. Chem. Soc.* **1957**, *79*, 1439–1441. b) *Atlas of Electron Spin Resonance Spectra* (Eds.: B. H. J. Bielski, J. M. Gebicki), Academic Press, NY, **1967**, p. 198.

[25] a) J. Fajer, D. C. Borg, A. Forman, D. Dolphin, R. H. Felton, *J. Am. Chem. Soc.* **1970**, *92*, 3451–3459. b) J. Fajer, D. C. Borg, A. Forman, R. H. Felton, L. Vegh, D. Dolphin, *Ann. N. Y. Acad. Sci.* **1973**, *206*, 349–364.

[26] R. S. Czernuszewicz, K. A. Macor, *J. Raman Spec.* **1988**, *19*, 553.

[27] D. Dolphin, R. H. Felton, D. C. Borg, J. Fajer, *J. Am. Chem. Soc.* **1970**, *92*, 743.

[28] E. T. Shimomura, M. A. Phillippi, H. M. Goff, W. F. Scholz, C. A. Reed, *J. Am. Chem. Soc.* **1981**, *103*, 6778–6780.

[29] a) Similar phenomena for electrochemically oxidized **4** and **7** were also observed by Ichimori et al. (ref. [21a]). b) The singlet observed for **6a** could simply be a result of a decrease in its a_N value due to electron density withdrawal by the chlorine substituents. But, because, for a singlet of this type, the ΔH_{pp} (3.0–2.6 G) hides five "unresolved" coupling constants ($4a_N$'s and the intrinsic linewidth, which must be $\geq a_N$), an upper limit for a_N would be 0.6 G. Since the values for **10a** and **5a** are 1.1–1.2 and 1.56 G, respectively, the above-mentioned suggestion is highly unlikely.

[30] H. Yamaguchi, M. Nakano, K. Itoh, *Chem. Lett.* **1982**, 1397–1400.

[31] X.-Y. Li, R. S. Czernuszewicz, J. R. Kincaid, P. Stein, T. G. Spiro, *J. Phys. Chem.* **1990**, *94*, 31–47.

[32] D. Steele, T. R. Nanney, E. R. Lippincott, *Spectrochim. Acta* **1966**, *22*, 849–859.

[33] J. H. S. Green, D. J. Harrison, W. Kynaston, *Spectrochim. Acta* **1971**, *27A*, 793–806.

[34] G. Varsanyi, S. Szoke, *Vibrational Spectra of Benzene Derivatives*, Academic Press, New York, **1969**.

[35] B. B. Johnson, W. L. Peticolas, *Ann. Rev. Phys Chem.* **1976**, *27*, 465.

[36] G. Zerbi, S. Sandroni, *Spectrochim. Acta.* **1966**, *24a*, 483, 511.

[37] N. Fuson, C. Garrigou-Lagrange, M. L. Josien, *Spectrochim. Acta*, **1960**, *16*, 106–127.

[38] D. Lin-Vien, N. B. Colthup, W. G. Fateley, J. G. Grasselli, *The Handbook of Infrared and Raman Characteristic Frequencies of Organic Molecules*, Academic Press, San Diego, **1991**.

[39] S. Choi, T. G. Spiro, K. C. Langry, K. M. Smith, D. L. Budd, G. N. LaMar, *J. Am. Chem. Soc.* **1982**, *104*, 4345–4351.

[40] K. M. Kadish, *Prog. Inorg. Chem.* **1986**, 435–605.

[41] a) For a theoretical analysis of the UV/Vis spectra of metalloporphyrin radical cations, see: W. D. Edwards, M. C. Zerner, *Can. J. Chem.* **1985**, *63*, 1763–1772. b) For a recent analysis of the UV/Vis spectra of metalloporphyrins, see: D. H. Jones, A. S. Hinman, T. Ziegler, *Inorg. Chem.* **1993**, *32*, 2092–2095.

[42] a) M. Huber, T. Galili, K. Möbius, H. Levanon, *Israel J. Chem.* **1989**, *29*, 65–71. b) M. Huber, H. Kurreck, B. von Maltzan, M. Plato, K. Möbius, *J. Chem. Soc. Faraday Trans.* **1990**, *86*, 1087–1094.

[43] R. H. Felton in *The Porphyrins, Vol. 5* (Ed.: D. Dolphin), Academic Press, New York, **1978**, Chap. 3.

[44] W. A. Oertling, A. Salehi, Y. C. Chung, G. E. Leroi, C. K. Chang, G. T. Babcock, *J. Phys. Chem.* **1987**, *91*, 5887–5898.

[45] The Taft's steric and polar parameters of *ortho*-chloride and fluoride: E_s = 0.18 (*o*-Cl) and 0.49 (*o*-F), σ^* = 0.37 (*o*-Cl) and 0.41 (*o*-F) were taken from Table 2.2 and σ_R° = − 0.20 (Cl) and −0.35 (F), σ_m = 0.37 (*m*-Cl) from Tables 1.4 and 1.2 in *Advances in Linear Free Energy Relationships* (Eds.: N. B. Chapman, J. Shorter), Plenum Press, NY, **1972**.

[46] M. J. Crossley, L. D. Field, A. J. Forster, M. M. Harding, S. Sternhell, *J. Am. Chem. Soc.* **1987**, *109*, 341–348. S. S. Eaton, G. R. Eaton J. *Chem. Soc. Chem. Commun.* **1974**, 576–577.

[47] a) W. R. Scheidt, Y. J. Lee, *Structure and Bonding (Berlin)* **1987**, *64*, 1–70. b) W. R. Scheidt, J. U. Mondal, C. W. Eigenbrot, A. Adler, L. J. Radonovich, J. L. Hoard, *Inorg. Chem.* **1986**, *25*, 795. c) L. D. Spaulding, P. G. Eller, J. A. Bertnard, R. H. Felton, *J. Am. Chem. Soc.* **1974**, *96*, 982. d) K. M. Barkigia, L. D. Spaulding, J. Fajer, *Inorg. Chem.* **1983**, *22*, 34.

[48] M. W. Renner, R.- J. Cheng, C. K. Chang, J. Fajer, *J. Phys. Chem.* **1990**, *94*, 8508–8511, and references therein.

[49] For a comprehensive discussion of temperature effects on ESR hfc's in cases of two nearly degenerate states, see: M. T. Jones, *J. Phys. Chem.* **1978**, *82*, 1138 and ref. [14], pp. 250–251. In principle, the energy difference between the two states can be calculated with the aid of Equation (15) of ref. [14]. Assuming that the nitrogen coupling constants of the A_{2u} and A_{1u} states are 1.458 G (from **3a**) and 0.00 G, respectively, from the value a_N = 1.10 G of **10a** at − 90 °C, the calculated ΔE between the two states is 0.41 kcal mol^{-1}.

[50] For a similar effect of axial ligands on the electronic state of cobalt porphyrins, see ref. [16a].